

**Pb on Mo(110) studied by scanning tunneling microscopy**

A. Krupski\*

*Institute of Experimental Physics, University of Wrocław, pl. Maxa Borna 9, PL 50-204 Wrocław, Poland*  
(Received 26 February 2009; revised manuscript received 12 June 2009; published 21 July 2009)

Scanning tunneling microscopy (STM) has been used to investigate the growth behavior of ultrathin Pb films on the Mo(110) surface at room temperature. The analysis of STM measurements indicates that for a coverage  $\theta < 1$  ML two-dimensional growth of the first Pb monolayer (wetting layer) took place. Above  $\theta > 1$  ML, the three-dimensional growth of the Pb islands with strongly preferred atomic scale “magic height” and flat top is observed. At coverages between  $1 \text{ ML} < \theta \leq 2 \text{ ML}$ , only islands containing two atomic layers of Pb are observed. At coverages between 2 and 3 ML, islands containing two and four atomic layers of Pb are observed. At higher coverages  $\theta > 3 \text{ ML}$ , the island height distribution shows peaks at relative heights corresponding to  $N = (2, 4, 6, 7, \text{ and } 9)$  of Pb atomic layers.

DOI: [10.1103/PhysRevB.80.035424](https://doi.org/10.1103/PhysRevB.80.035424)

PACS number(s): 68.37.Ef, 68.35.bd, 68.43.-h

**I. INTRODUCTION**

Ultrathin epitaxial film systems exhibit a variety of interesting properties owing to the strong correlation between the electronic structure of the film and its morphology, strain, and defect structure.<sup>1,2</sup> Acknowledge of the structures of face-centered-cubic (fcc) thin metal films on body-centered-cubic (bcc) metals is important for understanding the initial growth of these adsorption systems. Structural studies of the fcc/bcc systems provide a great deal of information on the connection between geometrical properties of the adsorbed atomic layers and the atomic arrangements of the substrates. Until now, the surface structures and growth mode of various adsorbate metals on the Mo(110) substrate have been investigated by the use of different experimental and theoretical methods in a number of works (e.g., Pb,<sup>3,4</sup> Sn,<sup>5,6</sup> Cu,<sup>7</sup> Co,<sup>8</sup> Fe,<sup>9</sup> Ni,<sup>10</sup> Mg,<sup>11</sup> Ba,<sup>12</sup> K,<sup>13</sup> S,<sup>14</sup> Ag,<sup>6,15</sup> Au,<sup>6,16</sup> In,<sup>6,17</sup> etc.). Recently, the oxide formation on transition-metal surfaces has also received considerable attention,<sup>18–21</sup> including Mo(110) surface.<sup>22,23</sup>

The adsorption of Pb on Mo(110) surface has been investigated experimentally.<sup>3,4</sup> The initial investigation of this system was by Tikhov and Bauer<sup>3</sup> using the combination of low-energy electron diffraction (LEED), Auger electron spectroscopy (AES), work-function change measurements ( $\Delta\Phi$ ) and thermal-desorption spectroscopy (TDS) at a substrate temperature of about 350 K. In the submonolayer range, attractive lateral interactions in the lead layer were found. After completion of one monolayer (ML), three-dimensional growth was observed. Between Pb and Mo at any coverage and temperature, alloying was not observed. Finally, the authors proposed a set of models of the ordered superstructures formed by lead on the Mo(110) face at different coverages. Jo *et al.*<sup>4</sup> studied surface structures of lead deposited on Mo(110) surface by means of reflection high-energy electron diffraction and scanning electron microscopy with respect to the film thickness and substrate temperature. The authors observed four kinds of surface structures. Three of them appeared at nearly one monolayer of lead coverage at room temperature. The growth modes of Pb/Mo(110) adsorption system are Frank–van der Merwe growth mode (layer by layer) at room temperature and Stranski-Krastanov

growth mode at high temperature. I present room-temperature scanning tunneling microscopy (STM) investigations of the growth of lead layers on the Mo(110) surface with a thickness ranging from 0.4 ML to approximately 5 ML.

**II. EXPERIMENT**

The measurements were carried out in a metal ultra-high-vacuum chamber with a base pressure of  $2 \times 10^{-10}$  mbar. The chamber was equipped with reverse-view LEED optics, which were used for AES and LEED measurements, and also with an Omicron variable-temperature STM. The Mo(110) crystal was mounted on a home-built transferable sample holder with an integrated electron-beam heater. The sample could be heated to 2400 K. The crystal temperature was measured with a W5%Re–W26%Re thermocouple. The Mo(110) crystal was cleaned by repetitive flashing ( $30 \times 5$  min) at 1200 K in  $p = 3 \times 10^{-7}$  mbar oxygen atmosphere to remove the residual carbon contamination. Oxygen was removed by flashing the sample at 2400 K for 15 s. The flashing at 2400 K was repeated before each experiment. This procedure was repeated until the carbon peak became invisible in AES spectrum and a LEED pattern of the clean Mo(110) face with sharp spots and low background was obtained. Lead (99.999%) was evaporated onto the crystal surface from a quartz crucible surrounded by a tungsten resistive heater in a vacuum of  $5.0 \times 10^{-10}$  Torr or better, and at a deposition rate of  $1.67 \times 10^{-3}$  ML/s. Film coverages are described in MLs, where a 1 ML Pb film corresponds to an atomic packing density of  $9.40 \times 10^{14}$  atoms/cm<sup>2</sup>. All STM measurements were performed at room temperature with W tips, in constant current mode. STM data were processed by freeware image-processing software.<sup>24</sup>

**III. RESULTS AND DISCUSSION**

Figure 1 shows STM images from the Mo(110) surface with different Pb coverages in order to illustrate the morphology of the Pb layers deposited on Mo at room temperature. Figure 1(a) displays the STM image, taken on low-index Mo(110) substrate with terraces between 100 and

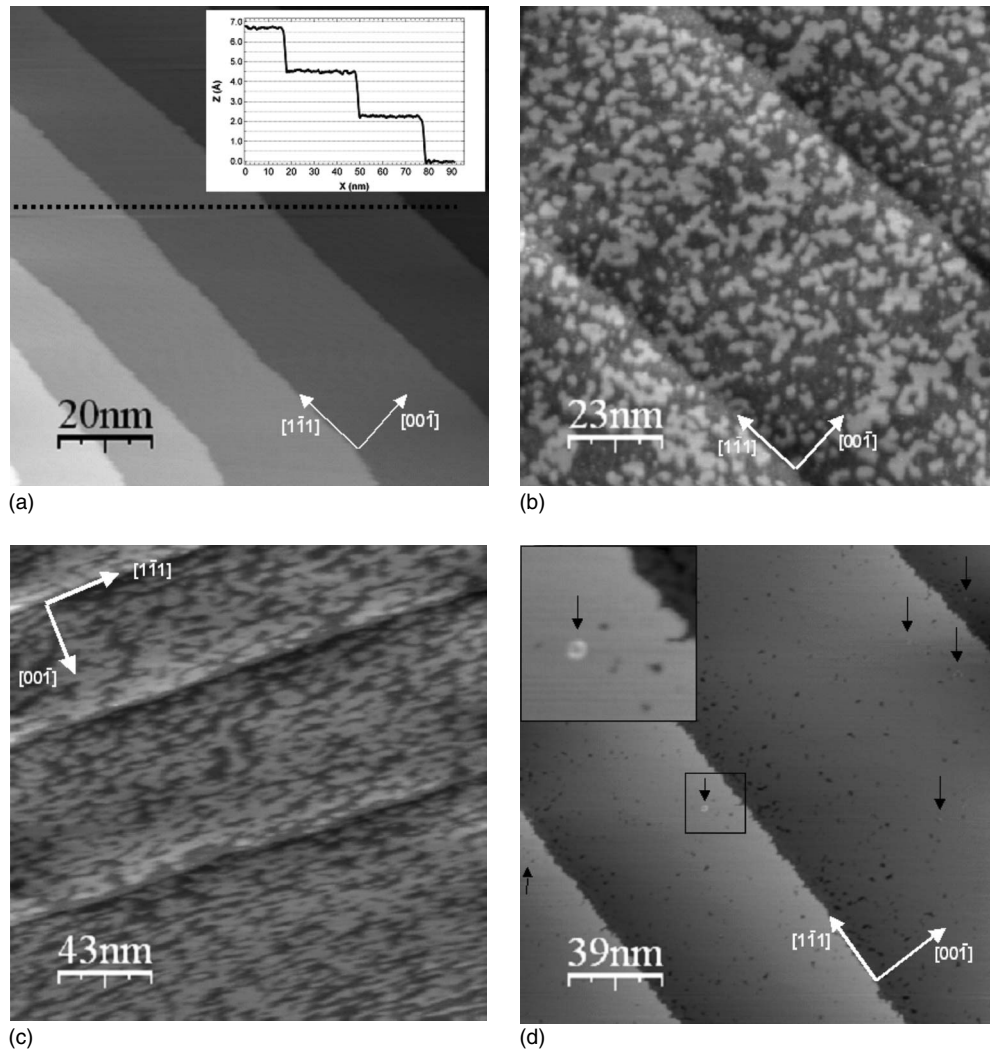


FIG. 1. STM images of Pb deposited on Mo(110) at  $T=300$  K at coverage  $\theta \leq 1.0$  ML: (a) clean Mo(110) ( $1000 \times 1000 \text{ \AA}^2$ ,  $I_T = 0.8$  nA, and  $U_{\text{bias}} = 100$  mV). The line scan shown in the inset evidences terraces approximately between 100 and 400  $\text{\AA}$  wide, (b) 0.4 ML ( $1140 \times 1140 \text{ \AA}^2$ ,  $I_T = 0.2$  nA, and  $U_{\text{bias}} = 1$  V), (c) 0.8 ML ( $2159 \times 2159 \text{ \AA}^2$ ,  $I_T = 0.2$  nA, and  $U_{\text{bias}} = 1$  V), (d) 1.0 ML ( $1951 \times 1951 \text{ \AA}^2$ ,  $I_T = 0.3$  nA, and  $U_{\text{bias}} = 800$  mV). The inset presents zoom ( $242 \times 242 \text{ \AA}^2$ ) in the area indicated by a square. Arrows indicate the places where the Pb atoms of the second layer start to nucleate at dislocations of the first Pb layer.

400  $\text{\AA}$  wide separated by monoatomic steps aligned along the  $[1\bar{1}1]$  direction. The height of the steps on the Mo(110) surface was measured by STM to be  $2.3 \pm 0.2 \text{ \AA}$ . Figure 1(b) shows a typical STM image for 0.4 ML Pb deposition. The bright features represent Pb islands with an irregular shape. These are monolayer height islands. As the Pb coverage is increased to 0.8 ML, the lead islands coalesce, resulting in larger and more irregular islands, as may be seen in Fig. 1(c). As the Pb coverage is close to 1 ML, the Pb wets the Mo(110) surface almost completely, as can be seen in Fig. 1(d). This is not easy to confirm with STM or adsorbate wets the surface or not. However, the reason for the almost perfect wetting is because of the high-specific surface free energy of the Mo(110) surface as compared with that of the Pb(111) surface. Since the total specific surface free energy should be minimized, a covered Mo(110) surface is favored. As one can see in the inset of Fig. 1(d), the first Pb layer on the Mo(110) surface is not free from dislocation defects. The

pseudomorphic growth of the first two-dimensional Pb layer is thermodynamically driven by the lower surface free energy of Pb ( $\gamma_{\text{Pb}} = 0.6 \text{ J/m}^2$ ) compared with Mo ( $\gamma_{\text{Mo}} = 2.95 \text{ J/m}^2$ ) (Ref. 25) so that the Pb layer wets the Mo surface despite the elastic energy required as a result of the large lattice mismatch. Closer inspection of Fig. 1(d) shows that the second lead layer starts to grow before the completion of formation of the first lead layer. The arrows in Fig. 1(d) indicate the places where the Pb adatoms of the second layer start to nucleate<sup>26,27</sup> at dislocation defects of the first Pb layer. As we can see, the density of the dislocation defects is higher at monoatomic ledges. At higher coverages ( $1 \text{ ML} < \theta \leq 5 \text{ ML}$ ) the growth seems to be three dimensional (Stranski-Krastanov), as can be seen in Figs. 2 and 3. These results contradict the literature data,<sup>4</sup> where layer-by-layer (Frank-van der Merwe) growth at room temperature was reported. Figures 2(a) and 2(c) show STM images after 1.2 and 1.5 ML of Pb were deposited on the Mo(110) surface at RT. Height profiles taken across the Pb islands [Fig. 2(b)] show

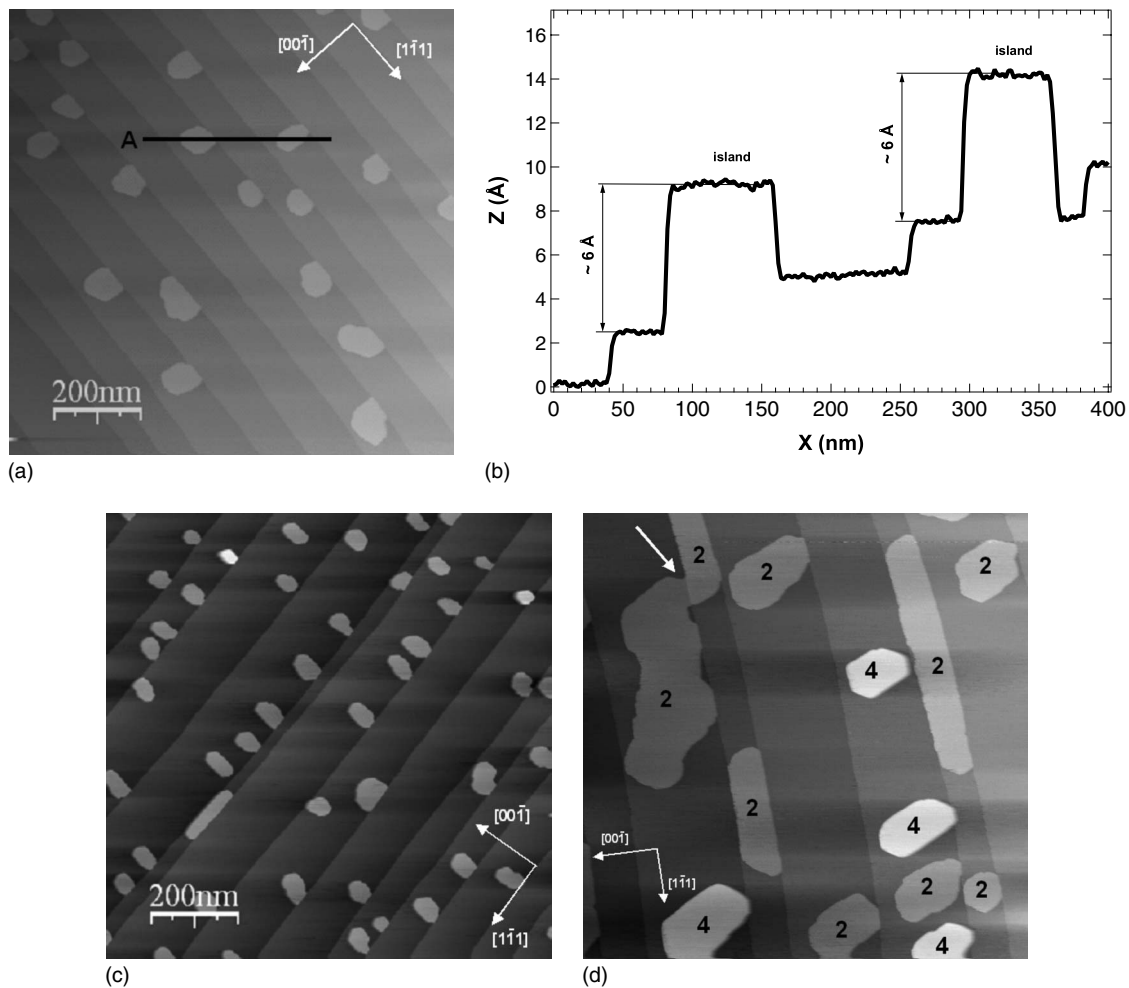


FIG. 2. STM images of Pb deposited on Mo(110) at  $T=300$  K at coverage  $1 \text{ ML} < \theta \leq 4 \text{ ML}$ . The height of Pb islands is measured from the wetting layer: (a) 1.2 ML ( $10\,000 \times 10\,000 \text{ \AA}^2$ ,  $I_T=0.2$  nA, and  $U_{\text{bias}}=1$  V), (b) Height profile along the line A from the image in (a) demonstrating that the height of the islands corresponds to the height of a double Pb step height, (c) 1.5 ML ( $10\,000 \times 10\,000 \text{ \AA}^2$ ,  $I_T=0.2$  nA, and  $U_{\text{bias}}=800$  mV). Inset presents differentiated STM image to enhance the contrast. (d) 2.5 ML ( $8563 \times 8563 \text{ \AA}^2$ ,  $I_T=0.2$  nA, and  $U_{\text{bias}}=1.0$  V). The height of the Pb islands corresponds to 2 and 4 atomic layers of Pb(111).

that the Pb crystallites have a thickness of about  $6 \text{ \AA}$ . The interlayer spacing along the  $[111]$  direction of Pb is  $d_{111}=2.86 \text{ \AA}$  and therefore the islands have a thickness corresponding to the stacking of two atomic layers. The height of Pb islands is measured from the wetting layer. For coverages below 2 ML, Pb islands with an average diameter of  $800 \text{ \AA}$  with a standard deviation of  $70 \text{ \AA}$  are observed. As the Pb coverage is increased up to 2.5 ML [Fig. 2(d)], more than 75% of the islands are two layers in height. Four-layer high islands are also observed, however, but they represent less than 25% of the total population of the Pb islands. In Fig. 2(d), the heights of the Pb islands in atomic layers are indicated. The arrow in Fig. 2(d) points to Pb islands which extend over two terraces of the substrate, with their thickness changing by 1 ML from terrace to terrace. This shape has been termed an “atomic wedge.”<sup>28</sup> The observed Pb islands on the wetting layer have regular shapes, sharp edges, and smooth tops, and tend to grow up with higher coverages, suggesting that such islands are stable. It should be pointed out that above  $\theta > 1$  ML, one-layer-thick Pb islands were never observed. For coverages greater than 3 ML [Fig. 3(a)],

further formation of islands with sharp edges and smooth tops is observed. The island height distribution (number of Pb islands with a given height), however, shows strong peaks at the relative heights corresponding to the number ( $N=2, 4$ , and 6) of Pb atomic layers [see Fig. 3(b)]. The arrows in Fig. 3(b) denote the most abundant island heights (“magic heights”) in Fig. 3(a) at coverage of 5 ML. A similar peculiar behavior of Pb adlayers was observed on Si(111) surfaces (see, e.g., Refs. 29–32) and is still the subject of lively discussion about the origin of this effect. A coverage of Pb under 5 ML deposited on Si(111) at a temperature between 170 and 250 K typically results in the formation of Pb islands of ( $N=4, 5, 6, 7$ , and 9) atomic layers in height above the wetting layer. Nevertheless, the occurrence of magic heights reveals a special stability associated with islands of specific thickness. Uniform island height selection during metal thin-film growth has been observed in several systems and interpreted in terms of quantum size effects.<sup>33,34</sup> Typically, these electronic effects are observed on semiconductor [e.g., Pb, Ag, or Bi on Si(111),<sup>29–31,35–37</sup> Ag on GaAs(110) (Ref. 38)] or metal substrates [e.g., Ag/Fe(100) (Ref. 39) or

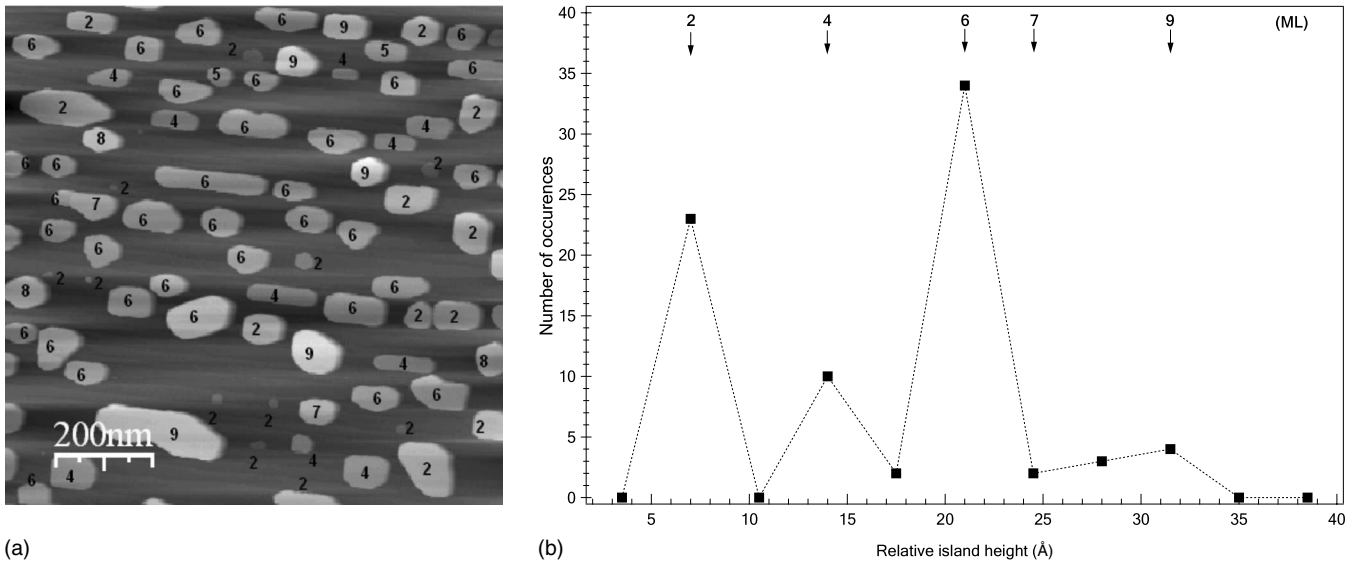


FIG. 3. (a) STM image of Pb deposited on Mo(110) at  $T=300$  K at coverage  $\theta=5$  ML ( $10\,000 \times 10\,000 \text{ \AA}^2$ ,  $I_T=0.2$  nA, and  $U_{\text{bias}}=1$  V). (b) Island height distribution (number of Pb islands with a given height) obtained from the image in (a), showing the strongly preferred heights of the Pb islands corresponding to two, four, and six atomic layers of Pb(111).

Pb/Cu(111) (Refs. 40–42)]. STM and scanning tunneling spectroscopy observations of Pb islands on the Cu(111) surface face<sup>40</sup> indicate that in the equilibrium distribution of island heights some heights appear much more frequently than others. “Magic” preferred heights correspond to islands with a quantum well state far from the Fermi energy while the “forbidden” heights appear to be those that have a quantum well state close to the Fermi level. The preferred heights for Pb islands on Cu(111) for coverages up to 5 ML correspond to the number ( $N=4, 6, 8, 10$ , and 11) of Pb atomic layers. Recently, Ayuela *et al.*<sup>43</sup> studied quantum size effects of Pb overlayers using density-functional theory (DFT) calculations and analytical models. The authors demonstrated that the high stability of Pb islands on metallic or semiconductor substrates at even higher coverages is supported by an extra second quantum beat pattern in the energetics of the metal film as a function of the number of atomic layers. It seems that this pattern is triggered by the butterflylike shape of the Fermi surface of lead in the [111] direction and supports the detection of stable “magic islands” of greater heights than measured up to now. The most stable magic islands from this DFT study have heights corresponding to the number ( $N=2, 4, 6, 7, 9, 11, 13, 14, 16, 18, 20, \dots$ ) of lead atomic layers, which is in good agreement with the experimental STM results presented here.

#### IV. CONCLUSIONS

In summary, I have investigated the growth behavior of ultrathin Pb films on Mo(110) surfaces at room temperature by means of scanning tunneling microscopy. In accordance with the literature data,<sup>3,4</sup> two-dimensional growth of the first lead layer is observed. Above  $\theta>1$  ML, the three-dimensional growth of the Pb islands with strongly preferred atomic scale magic height and flat top is observed. At coverages between 1 and 2 ML, STM images show the growth of two-atomic lead islands on the first lead layer (wetting layer), instead of layer-by-layer growth reported in the literature.<sup>4</sup> At coverage between 2 and 3 ML, islands containing two and four atomic layers of Pb are observed. At higher coverage  $\theta>3$  ML island height distribution shows peaks at relative heights corresponding to  $N=(2,4,6,7, \text{ and } 9)$  of Pb atomic layers. The DFT calculations<sup>42</sup> suggest that these magic islands are energetically favorable. Further experimental and theoretical work is needed to study the electronic structure and stability of these uniform Pb magic islands on Mo(110), which could have implications for the engineering of stable materials and devices with nanometer-scale dimensions.

\*Corresponding author. FAX: +48-71-328-73-65; akrupski@ifd.uni.wroc.pl

<sup>1</sup>F. Himpsel, J. Ortega, G. Mankey, and R. Willis, *Adv. Phys.* **47**, 511 (1998).

<sup>2</sup>J. H. Larsen and I. Chorkendorff, *Surf. Sci. Rep.* **35**, 163 (1999).

<sup>3</sup>M. Tikhov and E. Bauer, *Surf. Sci.* **203**, 423 (1988).

<sup>4</sup>S. Jo, Y. Gotoh, T. Niski, D. Mori, and T. Gonda, *Surf. Sci.* **454-456**, 729 (2000).

<sup>5</sup>Y. Maehara, T. Kimura, H. Kawanowa, and Y. Gotom, *J. Cryst. Growth* **275**, e1619 (2005).

<sup>6</sup>A. Krupski (unpublished).

<sup>7</sup>H. Kawanowa, J. Suzuki, Y. Mahara, Y. Gotom, and R. Souda, *J. Cryst. Growth* **275**, e1615 (2005).

<sup>8</sup>A. Mikkelsen, L. Ouattara, and E. Lundgren, *Surf. Sci.* **557**, 109 (2004).

<sup>9</sup>S. Murphy, J. Osing, and I. V. Shvets, *Surf. Sci.* **547**, 139

- (2003).
- <sup>10</sup>S. Murphy, V. Usov, and I. V. Shvets, *Surf. Sci.* **601**, 5576 (2007).
- <sup>11</sup>T. Tamori, H. Kazanowa, and Y. Gotom, *Surf. Sci.* **601**, 4412 (2007).
- <sup>12</sup>S. Jo and Y. Gotom, *Surf. Sci.* **464**, 145 (2000).
- <sup>13</sup>Y. Maehara, H. Kazanowa, and Y. Gotom, *Surf. Sci.* **600**, 3575 (2006).
- <sup>14</sup>Y. G. Zhou, X. T. Zu, J. L. Nie, and H. Y. Cio, *Chem. Phys.* **353**, 109 (2008).
- <sup>15</sup>E. Bauer and H. Poppa, *Thin Solid Films* **121**, 159 (1984).
- <sup>16</sup>J. A. Rodriguez and M. Kuhn, *Surf. Sci.* **330**, L657 (1995).
- <sup>17</sup>A. Katoh, H. Miwa, Y. Maehara, H. Kazanowa, and Y. Gotom, *Surf. Sci.* **566-568**, 181 (2004).
- <sup>18</sup>J. Gustafson, A. Mikkelsen, M. Borg, E. Lundgren, L. Kohler, G. Kresse, M. Schmid, P. Varga, J. Yuhara, X. Torrelles, C. Quiros, and J. N. Andersen, *Phys. Rev. Lett.* **92**, 126102 (2004).
- <sup>19</sup>J. Gustafson, A. Mikkelsen, M. Borg, J. N. Anderson, E. Lundgren, C. Klein, W. Hofer, M. Schmid, P. Varga, L. Kohler, G. Kresse, N. Kasper, A. Stierle, and H. Dosch, *Phys. Rev. B* **71**, 115442 (2005).
- <sup>20</sup>C. T. Campbell, *Phys. Rev. Lett.* **96**, 066106 (2006).
- <sup>21</sup>M. Todorova, W. X. Li, M. V. Ganduglia-Pirovano, C. Stampfl, K. Reuter, and M. Scheffler, *Phys. Rev. Lett.* **89**, 096103 (2002).
- <sup>22</sup>K. Radican, N. Berdunov, G. Manai, and I. V. Shvets, *Phys. Rev. B* **75**, 155434 (2007).
- <sup>23</sup>A. Okada, M. Yoshimura, and K. Ueda, *Surf. Sci.* **601**, 1333 (2007).
- <sup>24</sup>wsXM, <http://www.nanotec.es> (2009).
- <sup>25</sup>Q. Jiang, H. M. Lu, and M. Zhao, *J. Phys.: Condens. Matter* **16**, 521 (2004).
- <sup>26</sup>J. A. Venables, G. D. T. Spiller, and M. Hanbucken, *Rep. Prog. Phys.* **47**, 399 (1984).
- <sup>27</sup>H. Brune, *Surf. Sci. Rep.* **31**, 121 (1998).
- <sup>28</sup>I. B. Altfeder, K. A. Matveev, and D. M. Chen, *Phys. Rev. Lett.* **78**, 2815 (1997).
- <sup>29</sup>H. Hong, C. M. Wei, M. Y. Chou, Z. Wu, L. Basile, H. Chen, M. Holt, and T. C. Chiang, *Phys. Rev. Lett.* **90**, 076104 (2003).
- <sup>30</sup>W. B. Jian, W. B. Su, C. S. Chang, and T. T. Tsong, *Phys. Rev. Lett.* **90**, 196603 (2003).
- <sup>31</sup>Z. Kuntova, M. Hupalo, Z. Chvoj, and M. Tringides, *Surf. Sci.* **600**, 4765 (2006).
- <sup>32</sup>M. C. Tringides, M. Jałochowski, and E. Bauer, *Phys. Today* **60(4)**, 50 (2007).
- <sup>33</sup>T.-C. Chiang, *Surf. Sci. Rep.* **39**, 181 (2000).
- <sup>34</sup>M. Milun, P. Pervan, and D. P. Woodruff, *Rep. Prog. Phys.* **65**, 99 (2002).
- <sup>35</sup>V. Yeh, L. Berbil-Bautista, C. Z. Wang, K. M. Ho, and M. C. Tringides, *Phys. Rev. Lett.* **85**, 5158 (2000).
- <sup>36</sup>L. Huang, S. J. Chey, and J. H. Weaver, *Surf. Sci.* **416**, L1101 (1998).
- <sup>37</sup>T. Nagao, J. T. Sadowski, M. Saito, S. Yaginuma, Y. Fujikawa, T. Kogure, T. Ohno, Y. Hasegawa, S. Hasegawa, and T. Sakurai, *Phys. Rev. Lett.* **93**, 105501 (2004).
- <sup>38</sup>D. A. Evans, M. Alonso, R. Cimino, and K. Horn, *Phys. Rev. Lett.* **70**, 3483 (1993).
- <sup>39</sup>D.-A. Luh, T. Miller, J. J. Paggel, M. Y. Chou, and T.-C. Chiang, *Science* **292**, 1131 (2001).
- <sup>40</sup>R. Otero, A. L. Vazquez de Parga, and R. Miranda, *Phys. Rev. B* **66**, 115401 (2002).
- <sup>41</sup>E. Ogando, N. Zabala, E. V. Chulkov, and M. J. Puska, *Phys. Rev. B* **69**, 153410 (2004).
- <sup>42</sup>J. H. Dil, J. W. Kim, S. Gokhale, M. Tallarida, and K. Horn, *Phys. Rev. B* **70**, 045405 (2004).
- <sup>43</sup>A. Ayuela, E. Ogando, and N. Zabala, *Phys. Rev. B* **75**, 153403 (2007).